

# Equilibrium Swelling Behavior and Elastic Properties of Polymer–Clay Nanocomposite Hydrogels

Suzan Abdurrahmanoglu,<sup>1</sup> Volkan Can,<sup>2</sup> Oguz Okay<sup>2</sup>

<sup>1</sup>Department of Chemistry, Marmara University, Istanbul, Turkey

<sup>2</sup>Department of Chemistry, Istanbul Technical University, Istanbul, Turkey

Received 11 September 2007; accepted 23 April 2008

DOI 10.1002/app.28607

Published online 4 June 2008 in Wiley InterScience (www.interscience.wiley.com).

**ABSTRACT:** Nanocomposite hydrogels were prepared by free-radical polymerization of the monomers acrylamide (AAm), *N,N*-dimethylacrylamide (DMA), and *N*-isopropylacrylamide (NIPA) in aqueous clay dispersions at 21°C. Laponite XLS was used as clay nanoparticles in the hydrogel preparation. The hydrogels based on DMA or NIPA monomers exhibit much larger moduli of elasticity compared with the hydrogels based on AAm monomer. Calculations using the theory of rubber elasticity reveal that, in DMA-clay or NIPA-clay nanocomposites, both the effective crosslink density of the hydrogels and the functionality of the clay particles rapidly increase with increasing amount of Laponite up to 10% (w/v). The results sug-

gest that DMA-clay and NIPA-clay attractive interactions are stronger than AAm-clay interactions due to the formation of multiple layers on the nanoparticles through hydrophobic associations. It was also shown that, although the nanocomposite hydrogels do not dissolve in good solvents such as water, they dissolve in dilute aqueous solutions of acetone or poly(ethylene oxide) of molecular weight 10,000 g/mol, demonstrating the physical nature of the crosslink points. © 2008 Wiley Periodicals, Inc. *J Appl Polym Sci* 109: 3714–3724, 2008

**Key words:** nanocomposite hydrogels; clay; swelling; elasticity

## INTRODUCTION

Acrylamide (AAm)-based hydrogels are important materials of both fundamental and technological interests. These hydrogels are mainly obtained by free-radical crosslinking copolymerization of AAm in the presence of *N,N'*-methylenebis(acrylamide) (BAAm) as the crosslinker. Because the monomers are solid at the polymerization temperature, the reactions are necessarily carried out in an aqueous solution of the monomers. Polymer hydrogels formed in the presence of a diluent are, in general, soft and very brittle when handled in the swollen state. Most hydrogels of scientific and technological interest fall into this category, which limits their application areas.

Several attempts have been made in recent years to design hydrogels with improved mechanical properties.<sup>1–5</sup> The nanoscale dispersion of layered silicates or clays in polymer networks is one of the techniques offering significant enhancements in the material properties of hydrogels. Haraguchi et al. prepared such hydrogels starting from AAm-based

monomers together with Laponite as a physical crosslinker, replacing the traditional chemical crosslinker BAAm.<sup>6–9</sup> Laponite, a synthetic hectorite clay, when suspended in water forms disc-like particles with a thickness of 1 nm, a diameter of about 25 nm, and a negative surface charge density stabilizing dispersions in water.<sup>10,11</sup> The specific features of Laponite hydrogels are: (i) both the clay particles and the polymer chains are of comparable size and, (ii) the lack of internal flexibility of the clay particles compared to the polymer chains. These features allow the clay particles to align easier than the polymer chains and lead to the improved mechanical properties of the hydrogels. Formation of a crosslinked polymer network using a small amount of Laponite indicates that these nanoparticles act as a multifunctional crosslinker with a large effective functionality.<sup>12</sup> Contrary to the conventional chemically crosslinked hydrogels, the nanocomposite hydrogels formed using Laponite as a crosslinker exhibit extraordinary mechanical toughness, tensile moduli, and tensile strengths.<sup>6–9</sup> Recently, it was shown by rheological experiments that a large energy dissipation occurs during the deformation of the nanocomposite hydrogels that contain Laponite.<sup>13</sup> These results suggest that the polymer chains in the hydrogel are in a dynamic adsorption/desorption equilibrium with the clay particles, which requires an extensive rearrangement of the highly entangled polymer material close to the clay surface. This rearrangement during

Correspondence to: O. Okay (okay@itu.edu.tr).

Contract grant sponsor: Scientific and Technical Research Council of Turkey (TUBITAK); contract grant number: TBAG 105T246.

deformation is likely to equalize the force acting on the gel among the polymer chains, and, thus, is responsible for the excellent mechanical performance of these materials.

The goal of this study was to explore the influence of specific clay-polymer interactions on the macroscopic properties of nanocomposite hydrogels. We investigated the equilibrium swelling behavior and the elastic properties of nanocomposite hydrogels based on polyacrylamide (PAAm), poly(*N,N*-dimethylacrylamide) (PDMA), and poly(*N*-isopropylacrylamide) (PNIPA) as the hydrophilic polymer component and Laponite XLS as the clay component. As will be seen later, the properties of the hydrogels vary depending on the type of the monomer used in their preparation. The origin of this behavior is discussed on the basis of the results of the swelling and elasticity tests.

## EXPERIMENTAL

### Materials

AAM (Merck, Darmstadt, Germany), *N,N*-dimethylacrylamide (DMA, Aldrich), *N*-isopropylacrylamide (NIPA, Aldrich, Milwaukee, WI), BAAM (Merck), ammonium persulfate (APS, Merck), *N,N,N',N'*-tetramethylethylenediamine (TEMED, Merck), poly(ethylene oxide) (Fluka, Deisenhofen, Germany), and sodium chloride (Fluka) were used as received. The synthetic hectorite clay, Laponite XLS ( $\text{Na}_{0.7}^+[\text{Si}_8\text{Mg}_{5.5}\text{Li}_{0.3}\text{O}_{20}(\text{OH})_4]^{0.7-}$ , modified with pyrophosphate ions ( $\text{P}_2\text{O}_7^{4-}$ )) was provided by Rockwood (Cheshire, UK). Suspensions of Laponite XLS were prepared by dispersing the white powder at the preset concentrations in deionized water with vigorous stirring for 1 week.

### Polymerization

Nanocomposite hydrogels were prepared in a similar manner to that reported previously,<sup>13,14</sup> i.e., by free-radical polymerization of the monomers in aqueous clay suspensions using APS-TEMED redox initiator system at 21°C. The initial concentration of the monomer AAm, DMA, and NIPA was set to 5% (w/v) while the Laponite concentration was varied over a wide range. The monomer AAm, DMA, or NIPA and the accelerator TEMED (0.25%, v/v) were first dissolved in Laponite XLS aqueous suspensions. After bubbling nitrogen, the initiator APS (3.51 mM) was added to the reaction solution and the polymerization was conducted in plastic syringes of about 4 mm internal diameter for 24 h. In this way, several series of PAAm, PDMA, and PNIPA hydrogels were prepared at various clay contents. For the light scattering measurements, the solution was filtered

through Nylon membrane filters with a pore size of 0.2 μm and transferred in light scattering vials.

### Extraction of clay particles

The Laponite concentration in the gel network was determined by the extraction of the hydrogels in an excess of water and then drying the insoluble material to constant mass. The details were described elsewhere.<sup>14</sup> Within the limits of experimental error of about 8%, clay concentration inside the PDMA and PNIPA hydrogels was found to be equal to that in the reaction solution over the range of concentration investigated. For PAAm hydrogels with more than 7% Laponite, however, only about 60% of clay present in the comonomer feed remained inside the gel network after extraction.

### Swelling measurements

The nanocomposite hydrogels formed in syringes of about 4 mm internal diameter were cut into samples of about 10 mm length. Then, each sample was placed in an excess of water at 21°C ± 0.5°C. To reach swelling equilibrium, the hydrogels were immersed in water for at least 1 month replacing water several times. The swelling equilibrium was tested by weighing the gel samples. The gel volume change during the course of swelling was also monitored by measuring the diameter of the gel samples by using an image analyzing system consisting of a microscope (XSZ single Zoom microscope), a CDD digital camera (TK 1381 EG), and a PC with the data analyzing system Image-Pro Plus. To achieve good precision, five measurements were carried out on samples of different length taken from the same gel. Swelling measurements were also carried out in aqueous NaCl solutions of concentrations ranging from 10<sup>-5</sup> to 1.0M. The hydrogels with equilibrium swollen in water were transferred to vials containing the most diluted aqueous NaCl solution. The gel samples were allowed to swell in the solution for 2 weeks, during which aqueous NaCl was refreshed to keep the concentration as needed. After the swelling equilibrium is established, the gel samples were transferred into the next concentrated NaCl solution.

The interpretation of the swelling measurements in water was made on the basis of the relative weight  $m_{\text{rel}}$ , and the relative volume swelling ratios of gels  $V_{\text{rel}}$ , which were calculated as

$$m_{\text{rel}} = m_w/m_0 \quad (1a)$$

$$V_{\text{rel}} = (D_w/D_0)^3 \quad (1b)$$

where  $m_w$  and  $D_w$  are the mass and the diameter of the equilibrium swollen gel sample in water,  $m_0$  and

$D_o$  are their mass and diameter after preparation, respectively. The swelling results in salt solutions were presented in terms of the gel mass normalized with respect to the swollen gel mass in water,  $m_s/m_w$ , where  $m_s$  is the mass of the gel sample in salt solution. The swelling measurements in aqueous solutions of acetone and poly(ethylene oxide) (PEO) as well as the temperature-dependent swelling tests of the nanocomposite PNIPA hydrogels were carried out as described earlier.

### Elasticity tests

Uniaxial compression measurements were performed on nanocomposite hydrogels just after their preparation as well as in their equilibrium swollen states. All the mechanical measurements were conducted in a thermostated room of  $21^\circ\text{C} \pm 0.5^\circ\text{C}$ . The stress–strain isotherms were measured by using an apparatus previously described.<sup>15,16</sup> Briefly, a cylindrical gel sample of about 4 mm in diameter and 10 mm in length was placed on a digital balance (Sartorius BP221S; readability and reproducibility: 0.1 mg). A load was transmitted vertically to the gel through a rod fitted with a PTFE end-plate. The compressional force acting on the gel was calculated from the reading of the balance. The resulting deformation was measured after 20 s of relaxation by using a digital comparator (IDC type Digimatic Indicator 543-262, Mitutoyo Co., Kanagawa, Japan), which was sensitive to displacements of  $10^{-3}$  mm. The measurements were conducted up to about 15% compression. It should be noted that, compared with the chemical hydrogels with completely reversible stress–strain isotherms,<sup>15,16</sup> nanocomposite hydrogels exhibited considerable irreversibility, probably due to irrecoverable sliding of the chains over the surfaces of the clay particles upon being strained. However, from repeated measurements with several (at least three) fresh gel samples, the standard deviations in the modulus value were found to be less than 3%. The elastic modulus  $G$  was determined from the slope of linear dependence,

$$f = G(\lambda - \lambda^{-2}) \quad (2)$$

where  $f$  is the force acting per unit cross-sectional area of the undeformed gel specimen, and  $\lambda$  is the deformation ratio (deformed length/initial length).

### Static light scattering measurements

For the static light scattering measurements from Laponite dispersions as well as from the reaction solutions, the scattered light intensities were measured at  $25^\circ\text{C}$  using a commercial multi-angle light scattering DAWN EOS (Wyatt Technologies, Santa Barbara,

CA) equipped with a vertically polarized 30 mW Gallium-arsenide laser operating at  $\lambda = 690$  nm and 18 simultaneously detected scattering angles. The light scattering system was calibrated against a toluene standard (Rayleigh ratio at 690 nm =  $9.78 \times 10^{-6}$  cm<sup>-1</sup>, DAWN EOS software). Dispersions of Laponite with concentration in the range of 0.2–4.5% (w/v) in water were prepared from dry Laponite RDS powder. The scattered light intensities were recorded from angles  $\theta = 14.5^\circ$  to  $152.5^\circ$  which correspond to the scattering vector  $q$  range  $3.1 \times 10^{-4}$  to  $2.4 \times 10^{-3}$  Å<sup>-1</sup>, where  $q = (4\pi n/\lambda) \sin(\theta/2)$ ,  $n$  is the refractive index of the medium.

## RESULTS AND DISCUSSION

### Laponite dispersion

Before we discuss the characteristics of polymer–clay nanocomposite hydrogels, it is appropriate to obtain some view of the corresponding primary system, namely the pure clay dispersions. Laponite clay has a structural negative charge which is neutralized by the Na<sup>+</sup> ions absorbed onto the surfaces of the crystals.<sup>10,11</sup> When dispersed in water, Laponite stacks gradually cleave into discrete disc-like particles. The electrical double layer forming on both sides of the dispersed Laponite particles causes the particles to repel each other so that dispersions of Laponite are stable at low concentrations [Fig. 1(A)]. Increasing the Laponite concentration above 2% reduces the osmotic pressure holding the Na<sup>+</sup> ions away from the particle surface, which causes the electrical double layer to thin and allow the positive charge on the edge of the particles to interact with negative surfaces of adjacent particles. This results in the formation of a “House of cards” structure and the dispersion system becomes a highly thixotropic gel [Fig. 1(B)]. The binding between the negatively charged face and the positively charged edge of the Laponite particles can be inhibited by the addition of pyrophosphate ions.<sup>10,11</sup> In this case, the edges of the Laponite discs modified by pyrophosphate are negatively charged so that the surfaces and edges of discs exhibit the same charge, leading to electrostatic repulsion among the discs and efficiently prohibiting the formation of a gel structure [Fig. 1(C)].

In this work, we used Laponite XLS, Laponite clay modified with pyrophosphate ions. Therefore, Laponite XLS can be easily dispersed in water up to about 10% concentration. When Laponite XLS powder is added to water and vigorously shaken, at concentrations below 5% (w/v) Laponite, the suspension becomes completely transparent in a few hours. However, further development of the dispersion process took place a relatively long time.<sup>13</sup> For example, Figure 2(A) shows the scattered light intensity

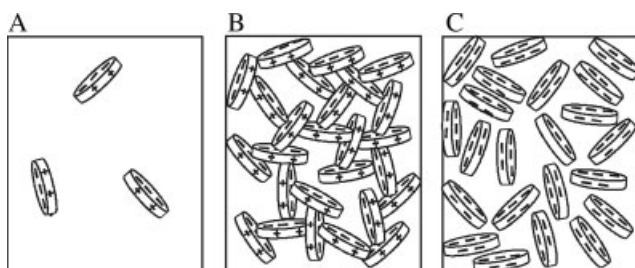


**Figure 1** Schematic representation of Laponite clay in various forms. (A) In dispersed state with a large amount of water. (B) In a gel state with a “House of cards” structure. (C) In dispersed state at a high Laponite concentration after treatment of the particles with pyrophosphate anions.

in terms of the Rayleigh ratio  $R(q)$  plotted against the square of the scattering vector  $q$  for a 2.5% (w/v) Laponite dispersion at various mixing times. It is seen that a strong upturn at low  $q$  appears at relatively short mixing times, indicating the presence of large agglomerates. However, at longer times, the upturn disappears and  $R(q)$  becomes almost independent of the scattering vector  $q$ .

After formation of stable Laponite dispersions, the monomer AAm, DMA, or NIPA and the redox initiator system APS/TEMED were added into the dispersion and the polymerization was conducted at 21°C. It was observed that, even at a very low Laponite concentration, the onset of the polymerization reactions is accompanied with the agglomeration of the nanoparticles. For example, Figure 2(B)

shows  $R(q)$  versus  $q^2$  plots recorded during the polymerization of AAm in a 0.3% (w/v) Laponite dispersion. It is seen that the upturn at low  $q$ , which disappeared during the preparation of clay dispersions [Fig. 2(A)], appears again with the onset of the reactions. This indicates formation of Laponite agglomerates before gelation due to the bridging effect of the polymer chains. Nie et al. recently observed two levels of organization characterized by two correlation lengths in PNIPA-Laponite nanocomposite hydrogels.<sup>12</sup> The smaller correlation length is of the same order of magnitude ( $10^1$  nm) as that observed in chemically crosslinked hydrogels, whereas the longer one around 200–250 nm is due to crosslinking via nanoparticles. It seems that this longer correlation length in nanocomposite hydrogels corresponds to the clusters of clay particles formed during their formation process.

### Elasticity of the hydrogels

After a reaction time of 1 day, the hydrogels were subjected to the elasticity tests, as described in the “Experimental” section. The filled symbols in Figure 3 show the moduli of elasticity  $G_0$  of the hydrogels just after their preparation plotted as a function of the Laponite concentration. The general trend is the increase in the modulus with increasing clay concentration. Further, at a fixed clay content, both PDMA and PNIPA hydrogels exhibit much larger elastic moduli compared with the PAAm hydrogels. PAAm hydrogels formed below 6% Laponite were too weak

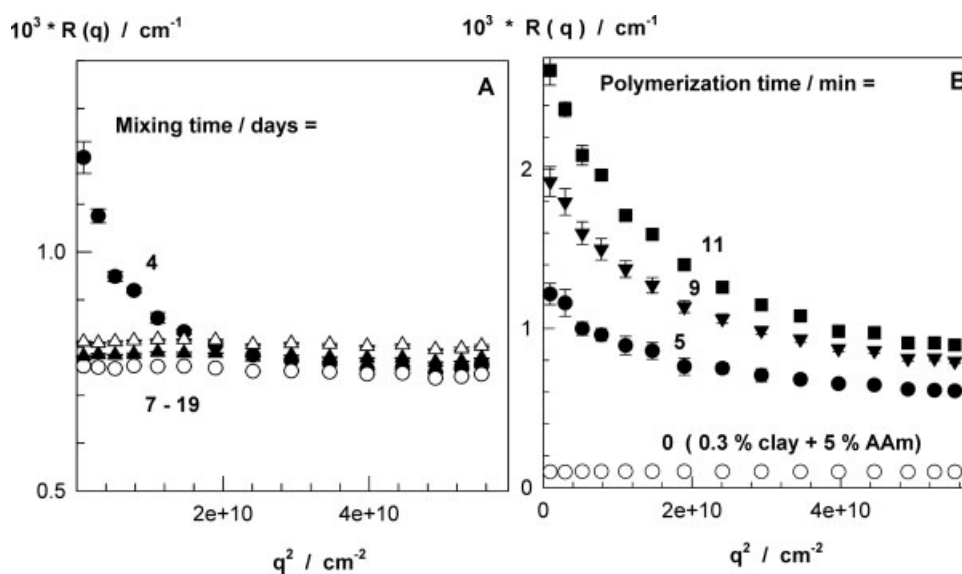


**Figure 2** (A) Scattered light intensity in terms of the Rayleigh ratio  $R(q)$  plotted against the square of the scattering vector  $q$  for a 2.5% (w/v) Laponite dispersion at various mixing times indicated in the figure. Note that the mixing times strongly depend on the rate and type of mixing. The data in the figure were obtained by shaking the Laponite–water mixture twice a day. (B)  $R(q)$  versus  $q^2$  plots during the polymerization of AAm in 0.3% (w/v) Laponite dispersion. Initial AAm concentration = 5% (w/v). Reaction times are indicated. The reaction cannot be monitored further due to large scattering at low  $q$  range which saturated the corresponding detector voltages.

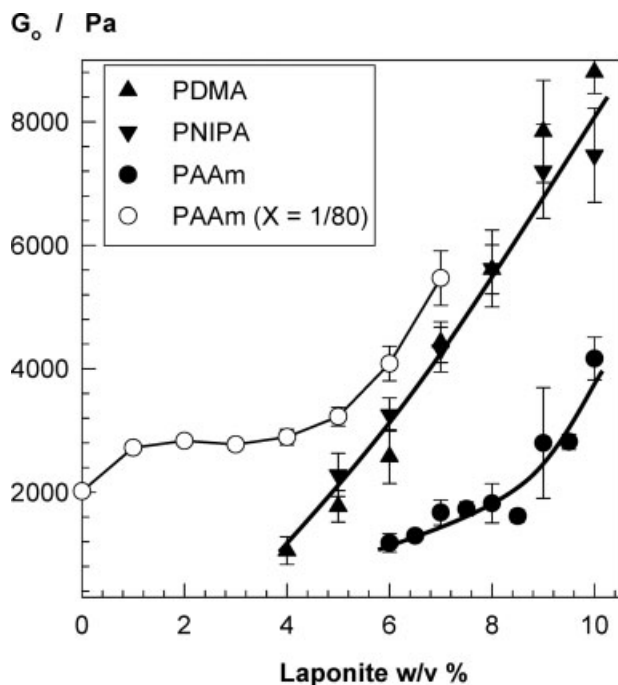


**Figure 3** Elastic modulus  $G_o$  of nanocomposite hydrogels just after their preparation plotted as a function of the Laponite concentration. The type of the hydrophilic polymer in the hydrogel is indicated.

to withstand the mechanical tests. Those obtained at higher Laponite contents exhibited elastic moduli in the range of 1–4 kPa, whereas the moduli of both PDMA and PNIPA hydrogels approached to 10 kPa at high Laponite contents.

To compare the crosslinker effect of Laponite with the chemical crosslinker BAAM, the polymerization of AAm was also carried out in the presence of both Laponite and BAAM. In this set of experiments, the crosslinker ratio  $X$  (mole chemical crosslinker BAAM/mol monomer AAm) was fixed at 1/80, while the Laponite concentration was varied between 0 and 7% (w/v). The results are also shown in Figure 3 by the open symbols. After an initial increase of 700 Pa, the modulus remains constant up to about 5% (w/v) Laponite, indicating that the chemical crosslinks mainly determine the rubber elasticity of the hydrogels. At higher Laponite contents, however,  $G_o$  rapidly increases with rising Laponite concentration so that the clay particles start to dominate the gel elasticity.

From the moduli of elasticity, one may calculate the effective crosslink density  $\nu_e$  of the hydrogels as well as the average functionality  $f_e$  of the clay particles. Assuming phantom network behavior, the elastic modulus  $G_o$  at the state of gel preparation is given by<sup>17,18</sup>

$$G_o = (1 - 2/f_e)\nu_e RTv_2^0 \quad (3)$$

where  $v_2^0$  is the volume fraction of crosslinked polymer in the gel,  $R$  and  $T$  are in their usual meanings. Furthermore, the average functionality  $f_e$  of the nanoparticles can be estimated from the molecular weight  $\bar{M}_w$  of Laponite as<sup>12</sup>

$$f_e = 2\nu_e v_2^0 \bar{M}_w / c \quad (4)$$

where  $c$  is the Laponite concentration in the hydrogel. Using the modulus data given in Figure 3 for the hydrogels without the chemical crosslinker BAAM, together with  $\bar{M}_w = 2.5 \times 10^6$  g/mol,<sup>9</sup>  $\nu_e$  and  $f_e$  of the nanocomposite hydrogels were calculated using eqs. (3) and (4). For calculations, we assumed complete conversion of the monomer to the crosslinked polymer.<sup>13,15,19,20</sup> The polymer densities  $\rho$  were taken as 1.35, 1.35, and 1.21 g/mL for PAAm, PNIPA, and PDMA, respectively.<sup>15,19</sup> The results are shown in Figure 4, where  $\nu_e$  and  $f_e$  are plotted against the Laponite concentration. The effective crosslink density  $\nu_e$  of both PDMA and PNIPA hydrogels rapidly increases with the clay content, whereas that of PAAm hydrogels only slightly increases. Further, the average functionality  $f_e$  of the nanoparticles, that is, the average number of effective network chains per particle increases with the clay concentration from 50 to 180 in PDMA and PNIPA hydrogels, which is much larger than the value found in PAAm hydrogels.

It should be pointed out that both  $\nu_e$  and  $f_e$  of PAAm hydrogels shown in Figure 4 are smaller than those reported earlier.<sup>13</sup> In Ref. 13 calculations were made using the modulus data of the hydrogels obtained from rheological measurements (by extrapolating the time-dependent elastic modulus  $G'$  to infinite reaction time). The different results thus obtained probably originate from the considerable irreversibility of stress-strain isotherms of nanocomposite hydrogels, as mentioned in the experimental section. Irreversibility in the isotherm is thought to be due to irrecoverable sliding of the chains over the surfaces of the clay particles upon being strained. Thus, the experimental setup for carrying out stress-strain measurements as well as the type of deformation affects the ability of the chains to slide along the particle surfaces.

The results suggest that both DMA-clay and NIPA-clay attractive interactions are stronger than AAm-clay interactions. It should be noted that the polymer-clay interactions are mainly hydrogen bonding interactions between adsorbed polymer molecules and clay surface. The polymer segments are bound to the surface of the clay particles due to hydrogen bonds between the surface oxygen atoms of clay and the amide protons of the polymer as well as between the surface hydroxyls and the carbonyl of the polymer. Considerable increase of the

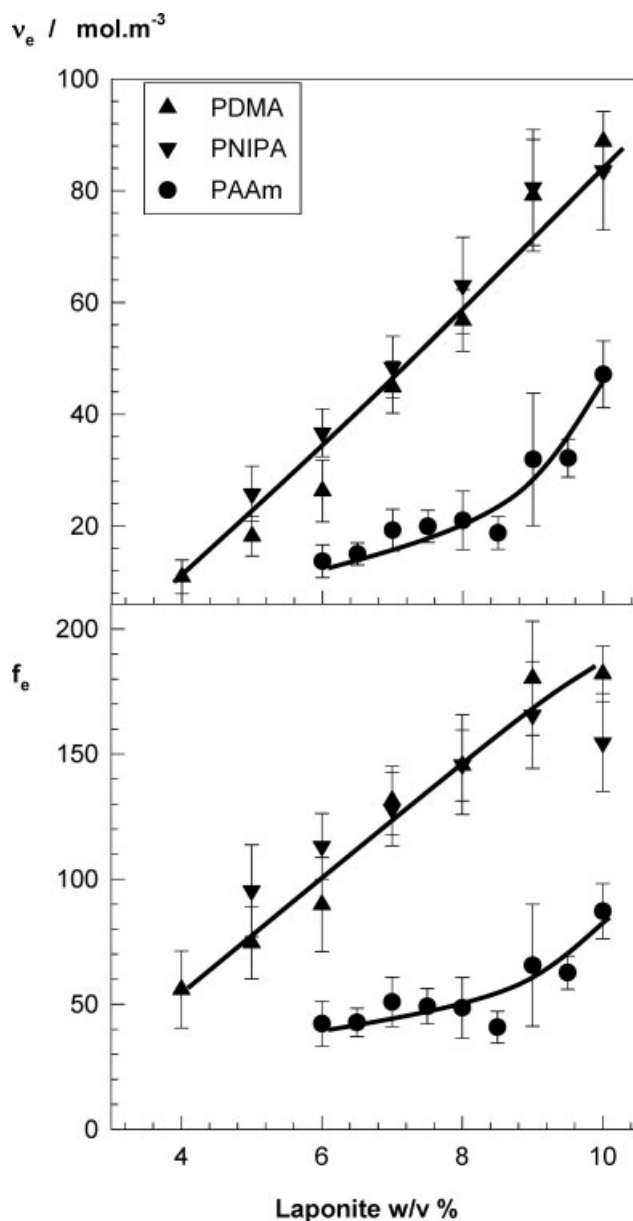


**Figure 4** The effective crosslink density  $v_e$  of the nano-composite hydrogels and the average functionality  $f_e$  of the clay particles shown as a function of the Laponite concentration. The type of the hydrophilic polymer in the hydrogel is indicated.

average functionality  $f_e$  of the clay particles with increasing Laponite concentration in both PDMA and PNIPA hydrogels suggests that more binding sites are available on the surface layer of the nanoparticles to interact with PDMA and PNIPA polymer chains compared with PAAm chains. It seems that hydrophobic modification of the hydrophilic PAAm increases the polymer-clay attractive interactions. Indeed, Aubry et al. showed that the amount of polymer adsorbed on the Laponite particles at surface saturation is about 30% lower for unmodified compared with the hydrophobically modified

(hydroxypropyl)guar samples.<sup>21</sup> Similar results were also reported by Argillier et al.<sup>22</sup> These authors investigated the adsorption of PAAm and hydrophobically modified PAAm chains on clay and silica in aqueous solutions. For the unmodified PAAm, a classical type of adsorption was reported, i.e., an initial increase in the adsorbed amount with polymer concentration and then a pseudoplateau which corresponds to the saturation of the surface by the polymer chains. However, for the hydrophobically modified PAAm, no plateau region was observed by the authors, but the adsorbed amount increased continuously with the concentration of polymer in the solution.<sup>22</sup> In accord with these findings, our result also shows a continuous increase of the functionality of clay with increasing clay concentration, if hydrophobically modified PAAm network chains are present in the reaction system. The result can be explained with the possible formation of multiple layers through hydrophobic associations. Thus, in PDMA or PNIPA hydrogels, the adsorbed layer on the nanoparticle is composed of chains which have segments in contact with the surface, and also, some chains which are not directly in contact with the surface but are linked through hydrophobic associations to other chains that are adsorbed on the surface. Increasing clay concentration also increases the number of layers on the particle surface so that both the functionality of the particles and the network crosslink density continuously increase in PDMA and PNIPA hydrogels.

### Swelling of the hydrogels

Equilibrium swelling measurements were conducted in water and in aqueous salt (NaCl) solutions. As reported recently, nanocomposite hydrogels containing Laponite exhibit unusual swelling behavior in water.<sup>14</sup> The volume or the mass of the hydrogels immersed in water rapidly increases and attains a maximum value after about 1 day. However, further increase in the swelling time results in the deswelling of the gels until they reach a limiting swelling ratio after about 5 days. This unusual swelling behavior occurring at clay concentrations above the overlap threshold  $c^*$  is due to the rearrangements of the highly entangled polymer chains and clay particles during the gel volume change.<sup>14</sup> In this work, all the data reported are equilibrium swelling values obtained after at least 1 month of swelling time in water.

For PAAm nanocomposite hydrogels, the swelling behavior was investigated between 0 and 10% (w/v) Laponite. Previous dynamic light scattering measurements as well as the rheological experiments showed formation of a PAAm hydrogel network at a Laponite content between 0.2 and 0.4% (w/v).<sup>13</sup> In con-

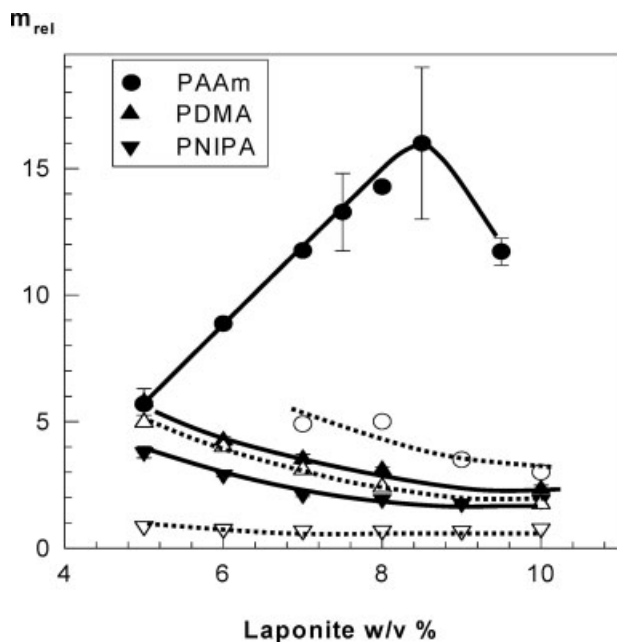


**Figure 5** The relative weight swelling ratio  $m_{rel}$  of the hydrogels (mass of swollen gel in water/mass of gel after preparation) plotted against the clay content. The type of the hydrophilic polymer in the hydrogel is indicated. Open symbols are the swelling data of the hydrogels in 1M NaCl solutions. Curves only show the trend of data.

trast, however, the reaction solutions containing less than 1.5% (w/v) Laponite dissolved completely in water after an immersion time of 1 week. This indicates that the three-dimensional network formed in this range of clay concentration is too weak to withstand the swelling pressure. At Laponite contents above 1.5% (w/v), PAAm hydrogels were obtained. However, those formed between 1.5 and 5% (w/v) Laponite were also too weak to withstand the swelling and elasticity tests. In this range of clay, the gel samples taken out of the solution cannot carry their own weight.

The filled symbols in Figure 5 show the weight swelling ratio  $m_{rel}$  of the hydrogels (mass of swollen gel/mass of gel after preparation) plotted against the clay content. For both PDMA and PNIPA hydrogels,  $m_{rel}$  decreases with the Laponite concentration. This is expected due to the action of Laponite as a crosslinking agent during gelation. Thus, the bonding of PDMA or PNIPA to clay particles is strong enough to suppress swelling of the network. However, for PAAm hydrogels,  $m_{rel}$  first increases up to about 8% (w/v) Laponite and then decreases. Because of the lower crosslinking efficiency of Laponite in AAm polymerization (Fig. 4), one may expect that the ionic osmotic pressure created due to the mobile ions on the particles is responsible for this behavior. To screen the charges in the gel network and thus, to visualize the swelling behavior of uncharged nanocom-

posite hydrogels, they were immersed in aqueous salt (NaCl) solutions of increasing NaCl concentration from  $10^{-5}$  to 1M. Figure 6 shows the normalized mass of PAAm hydrogels with three different clay contents plotted against NaCl concentration in the external solution. As usual in charged hydrogels,<sup>23</sup> the gel deswells with increasing salt concentration, indicating that increasing ionic strength screens the charges on the clay particles. This also demonstrates the ionic character of the hydrogels. Similar deswelling curves were also obtained for other hydrogel samples with various clay contents. In Figure 5, the open symbols connected by the dotted lines show  $m_{rel}$  versus Laponite % dependences for the hydrogels equilibrium swollen in 1M NaCl solution. The largest deswelling in salt solution occurs in PAAm hydrogels due to the relatively weak contribution of elastic osmotic pressure to the swelling process. Further, in concentrated salt solutions, the expected decrease of the swelling ratio with the Laponite content is observable for all the hydrogel samples.

### Charge density of the hydrogels

In this section, the swollen state properties of the nanocomposite hydrogels were analyzed using the theory of swelling equilibrium. According to the theory, the osmotic pressure  $\pi$  of a gel is the sum of three contributions<sup>17</sup>:

$$\pi = \pi_{mix} + \pi_{el} + \pi_{ion} \quad (5)$$

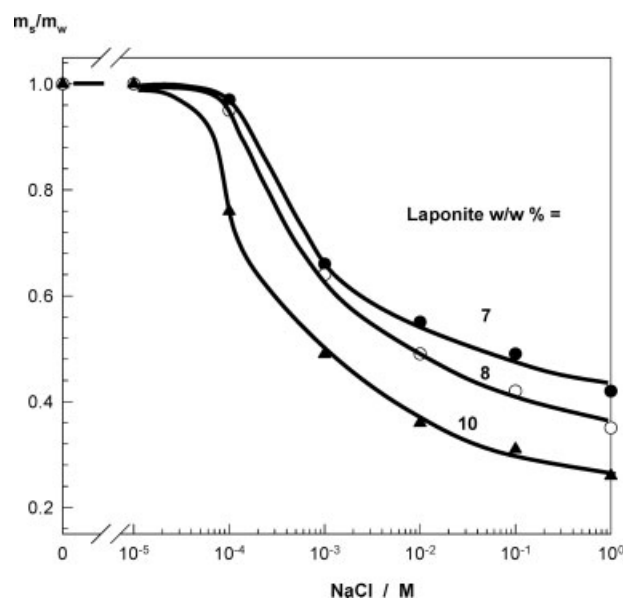


**Figure 6** The normalized mass  $m/m_w$  of PAAm hydrogels (mass of gel in salt solution/mass of gel in water) plotted against the NaCl concentration in the external solution. The type of the hydrophilic polymer in the hydrogel is indicated.  $X = 0$ . Laponite contents of the hydrogels are indicated.

where  $\pi_{\text{mix}}$ ,  $\pi_{\text{el}}$ , and  $\pi_{\text{ion}}$  are the osmotic pressures due to polymer-solvent mixing, due to deformation of network chains to a more elongated state, and due to the nonuniform distribution of mobile counterions between the gel and the solution, respectively. According to the Flory-Huggins theory,  $\pi_{\text{mix}}$  is given by<sup>17</sup>

$$\pi_{\text{mix}} = -\frac{RT}{V_1}(\ln(1-v_2) + v_2 + \chi v_2^2) \quad (5a)$$

where  $\chi$  is the polymer-solvent interaction parameter,  $V_1$  is the molar volume of solvent (18 g/mL), and  $v_2$  is the volume fraction of crosslinked polymer in the equilibrium swollen hydrogel. To describe the elastic contribution  $\pi_{\text{el}}$ , we will use the phantom network model for  $f_e$ -functional networks<sup>17,24</sup>:

$$\pi_{\text{el}} = -RT\left(1 - \frac{2}{f_e}\right)v_e v_2^{1/3} v_2^{2/3} \quad (5b)$$

Ionic contribution  $\pi_{\text{ion}}$  to the swelling pressure is caused due to the counterions on the surface of clay particles inside the gel network. When the gel is immersed in water, these ions cannot escape outside the gel due to the condition of electroneutrality. As a result, the concentration difference of the counterions between the gel and the outer solution (water) creates this additional ionic osmotic pressure, which is given by<sup>17</sup>

$$\pi_{\text{ion}} = CRT \quad (5c)$$

where  $C$  is the counterion concentration in the swollen gel, i.e.,

$$C = \frac{f_i}{V_1} v_2 \quad (5d)$$

where  $f_i$  is the effective charge density, i.e., the mole fraction of the charged units in the network chains that are effective in gel swelling.

Substitution of eqs. (5a)–(5d) into eq. (5) and because the osmotic pressure  $\pi$  equals to zero at swelling equilibrium, one obtains the following equation for equilibrium swollen nanocomposite hydrogels:

$$\ln(1-v_2) + v_2 + \chi v_2^2 + \left(1 - \frac{2}{f_e}\right)v_e V_1 v_2^{1/3} v_2^{2/3} - f_i v_2 = 0 \quad (6)$$

In the following, eq. (6) was solved for the effective charge density  $f_i$  of the hydrogels.  $\chi$  parameter values used were 0.480,<sup>25</sup> 0.485,<sup>15</sup> and  $0.47 + 0.36v_2$ <sup>19</sup> for PAAm-water, PNIPA-water, and PDMA-water systems, respectively. We assume that the Laponite particles do not affect the polymer-solvent interactions. Further, the polymer volume fraction  $v_2$  in the

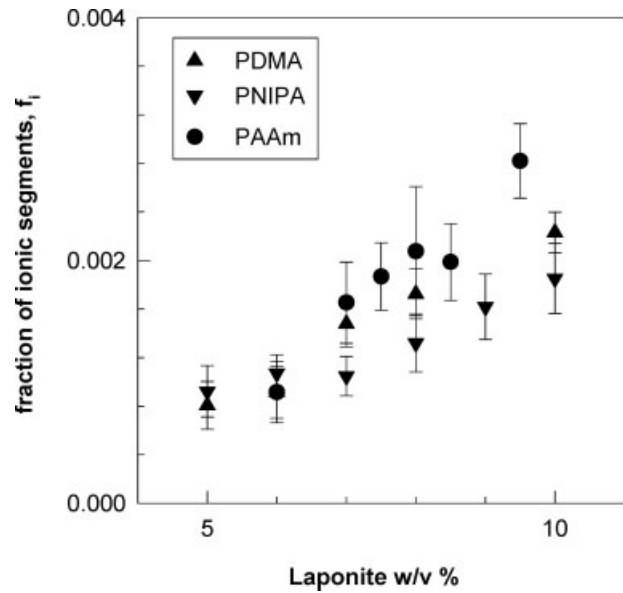


**Figure 7** The fraction of ionic segments  $f_i$  in nanocomposite hydrogels plotted against the Laponite content. The type of the hydrophilic polymer in the hydrogel is indicated.

equilibrium swollen hydrogel was calculated from the weight swelling ratio  $m_{\text{rel}}$  as

$$v_2 = \left(1 + \frac{(m_{\text{rel}}/c_M - 1)\rho}{d_1}\right)^{-1} \quad (6a)$$

where  $d_1$  is the density of water and  $c_M$  is the initial monomer concentration (0.05 g/mL). As both  $v_e$  and  $f_e$  are also known from the elasticity tests, one may solve eq. (6) for the remaining unknown  $f_i$ . Figure 7 shows the fraction of ionic segments  $f_i$  in nanocomposite hydrogels plotted against the Laponite content.  $f_i$  slightly increases from 0.1% up to about 0.2% with increasing amount of Laponite, and is almost independent on the type of the polymer. Because the unit cell of Laponite carries a negative charge of  $-0.7$ , one may calculate the theoretical charge density of the network chains as between 6 and 15%. Thus, only a small fraction of charges on the clay particles contributes to the gel swelling and most of the charges are not effective in the hydrogel swelling. A possible explanation is the close proximity of the charged groups on the particles which may lead to the condensation of the counterions.<sup>25</sup>

As is well known, PNIPA hydrogel is a typical temperature sensitive gel exhibiting a volume-phase transition in response to temperature changes.<sup>26</sup> Introduction of charged groups into the gel network affects the temperature induced volume-phase transition of nonionic PNIPA gels. Both the transition temperature and the extent of volume change during the transition increase with increasing charge density of PNIPA network. Because PNIPA nanocomposite



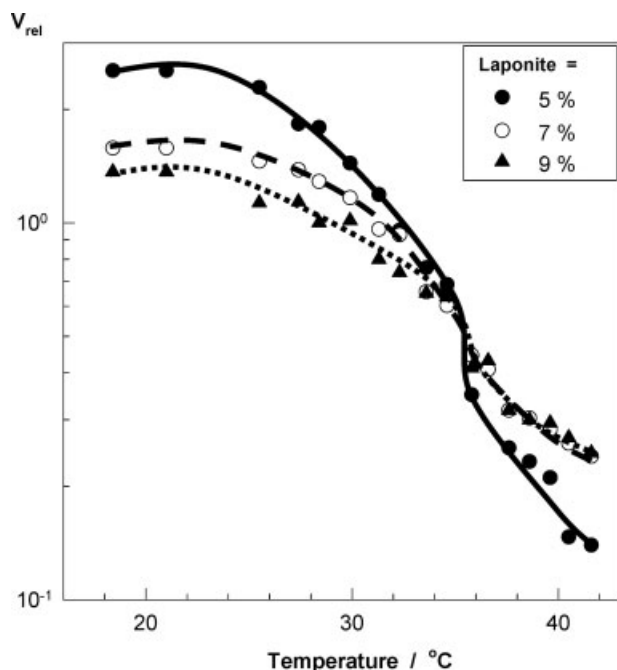


**Figure 8** The volume swelling ratio  $V_{rel}$  of PNIPA nanocomposite hydrogels plotted against the swelling temperature. The amount of Laponite in the hydrogels is indicated.

hydrogels also carry charged groups, they may exhibit a discontinuous volume phase transition on response to temperature. Figure 8 illustrates the dependence of the equilibrium volume swelling ratio  $V_{rel}$  of PNIPA hydrogels with 5–9% (w/v) Laponite on the swelling temperature. All the hydrogel samples undergo a volume-phase transition between swollen and collapsed states as the temperature is increased from 26 to 40°C. However, increasing clay content of the networks does not induce a substantial change in the swelling behavior of the hydrogels, except that the extent of the volume change is larger at low clay contents. It seems that the simultaneous increase of both the crosslink and charge densities with increasing amount of Laponite suppresses the extent of volume change during the transition region.

### Stability of the hydrogels

As Laponite nanoparticles produce physical crosslinks inside the hydrogel, these particles should be detached from the gel network under suitable conditions weakening the attractive interactions between the polymer segments and the particles. For example, addition of polar compounds such as salts to the Laponite dispersions reduces the osmotic pressure holding the  $\text{Na}^+$  ions away from the particle surface.<sup>27,28</sup> This causes the electrical double layer to thin, which should weaken polymer–clay interactions in favor of clay–clay interactions. However, all

the hydrogels remained stable in aqueous NaCl solutions over the whole range of concentration studied. In contrast, PAAm hydrogels immersed in aqueous acetone solutions containing 20–40% (v/v) acetone dissolved gradually indicating that the polymer bridges between the particles become unstable due to the thinning of the electrical double layer. At higher acetone contents, the gels remained in a collapsed state without any dissolution.

To elucidate the effect of acetone treatment on the properties of the nanocomposite PAAm hydrogels, we designed the following strategy: Two sets of PAAm hydrogels were prepared in the presence of the chemical crosslinker BAAM. The crosslinker ratio  $X$  was kept constant at 1/80. The hydrogel denoted by *A* was prepared in 7% (w/v) Laponite dispersion, while the hydrogel denoted by *B* was prepared in the absence of Laponite. Elasticity tests in their equilibrium swollen states in water gave the values 11 kPa and 1.7 kPa for the elastic moduli  $G$  of the hydrogels *A* and *B*, respectively. Thus, at 7% concentration, Laponite induces a sixfold increase in the elastic modulus of the swollen gel. This also means that, if the nanoparticles were completely removed from the gel network, a sixfold decrease in the elastic modulus of the hydrogel *A* should be observed. To check this point, swollen hydrogel samples *A* were immersed in aqueous acetone solutions of various amount of acetone for 1 month replacing the solution every other day. Then, the extracted hydrogels were immersed into water, and after attaining the equilibrium state, their moduli were measured. It was found that the gel samples immersed in 10 and 20% acetone by volume show a lower modulus  $G$  compared to the original hydrogel. The minimum value of  $G$  was measured as 6 kPa for the hydrogels extracted in 10% acetone solution. This means that not all but a part of the clay particles inside the gel could be removed by this extraction process.

Addition of water-soluble polymers also affects the properties of Laponite dispersions. It was shown that the binding between the particles can be inhibited by adding low molecular weight PEO due to the saturation of the particles with an adsorbed layer of polymer chains.<sup>11,29–31</sup> Indeed, we observed that, in aqueous solutions of PEO of molecular weight 10,000 g/mol, all the nanocomposite hydrogels (PAAm, PDMA, and PNIPA) dissolve, if the solutions contain 1% (w/v) PEO. To clarify this behavior, the hydrogel samples denoted by *A* and *B* were immersed in PEO solutions of various concentrations. After attaining the equilibrium state, their swelling ratios and elastic moduli were measured. Figures 9(A) and 9(B) show the variation of the elastic modulus  $G$  and the volume swelling ratio  $V_{rel}$  of the hydrogels equilibrium swollen in PEO solutions plotted against the PEO concentration in the external

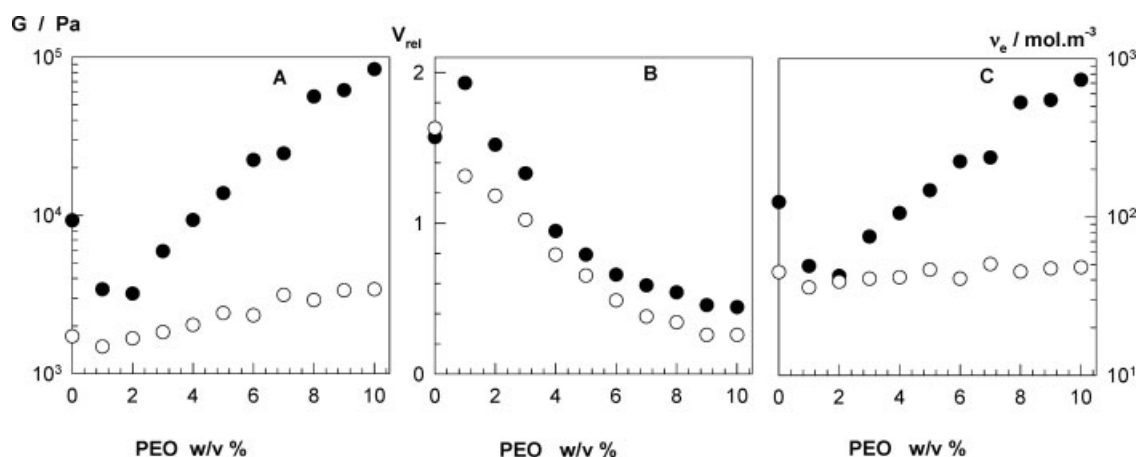


**Figure 9** The elastic modulus  $G$ (A), the volume swelling ratio  $V_{rel}$ , and the effective crosslink density  $v_e$  of PAAm hydrogels ( $X = 1/80$ ) with (7%, w/v, filled symbols) and without Laponite (open symbols).

solution. Filled symbols are for the hydrogels A (with 7% Laponite), whereas the open symbols are for those without Laponite (B). Using the experimental data together with the equation<sup>17,24</sup>:

$$G = (1 - 2/f_e)v_eRT(v_2^0)^{2/3}(v_2)^{1/3} \quad (7)$$

the effective crosslink densities  $v_e$  of the hydrogels were calculated. Note that the average functionality  $f_e = 4$  for the hydrogel B containing only BAAM crosslinker, whereas for the hydrogel A,  $f_e = 51$  (Fig. 4), neglecting the functionality of BAAM. The results are shown in Figure 9(C) for the hydrogels with (filled symbols) and without Laponite (open symbols) plotted against the PEO concentration. As expected, the crosslink density of the chemical gel (hydrogel B) remains unchanged in PEO solutions. For the hydrogel B containing Laponite, however, the crosslink density rapidly decreases and becomes equal to that of the conventional hydrogel A at 2% PEO, indicating that all the clay particles are disconnected from the gel network, i.e., they become ineffective for the rubber elasticity of the hydrogel. Thus, PEO chains entering in the gel phase cover the particles due to the strong PEO-clay interactions, so that the particles with an adsorbed layer of PEO chains lost their bridging ability between PAAm chains. Interestingly, further increase of PEO concentration increases the crosslink density of the hydrogels more than one order of magnitude compared to the initial crosslink density measured in water. The significant increase in the crosslink density at high PEO concentrations suggests formation of additional crosslinks in the nanocomposite hydrogel. One may speculate that PEO forms additional interparticle bridges between the particles so that the particles forming ineffective links are converted into elastically effective junction points.

## CONCLUSIONS

Nanocomposite hydrogels were prepared by free-radical polymerization of the monomers AAm, DMA, and NIPA in aqueous clay suspensions. Laponite XLS was used as clay nanoparticles in the hydrogel preparation. Nanocomposite hydrogels based on PDMA and PNIPA as the hydrophilic polymer component exhibit much larger moduli of elasticity compared to the hydrogels based on PAAm chains. It was shown that both the effective crosslink density of PDMA or PNIPA hydrogels and the functionality of the particles in these hydrogels rapidly increase with increasing amount of Laponite. The results suggest that DMA-clay and NIPA-clay attractive interactions are stronger than AAm-clay interactions due to the formation of multiple layers on the nanoparticles through hydrophobic associations. It was also shown that the nanocomposite hydrogels become unstable and dissolve in dilute aqueous solutions of acetone or PEO of molecular weight 10,000 g/mol.

## References

1. Tanaka, Y.; Gong, J. P.; Osada, Y. *Prog Polym Sci* 2005, 30, 1.
2. Gong, J. P.; Katsuyama, Y.; Kurokawa, T.; Osada, Y. *Adv Mater* 2003, 15, 1155.
3. Okumura, Y.; Ito, K. *Adv Mater* 2001, 13, 485.
4. Miquelard-Garnier, G.; Demoures, S.; Creton, C.; Hourdet, D. *Macromolecules* 2006, 39, 8128.
5. Huang, T.; Xu, H.; Jiao, K.; Zhu, L.; Brown, H. R.; Wang, H. *Adv Mater* 2007, 19, 1622.
6. Haraguchi, K.; Takehisa, T. *Adv Mater* 2002, 14, 1120.
7. Haraguchi, K.; Takehisa, T.; Fan, S. *Macromolecules* 2002, 35, 10162.
8. Haraguchi, K.; Farnworth, R.; Ohbayashi, A.; Takehisa, T. *Macromolecules* 2003, 36, 5732.
9. Haraguchi, K.; Li, H. J.; Matsuda, K.; Takehisa, T.; Elliott, E. *Macromolecules* 2005, 38, 3482.

10. Mongondry, P.; Tassin, J.-F.; Nicolai, T. *J Colloid Interface Sci* 2005, 283, 397.
11. Mongondry, P.; Nicolai, T.; Tassin, J.-F. *J Colloid Interface Sci* 2004, 275, 191.
12. Nie, J.; Du, B.; Oppermann, W. *Macromolecules* 2005, 38, 5729.
13. Okay, O.; Oppermann, W. *Macromolecules* 2007, 40, 3378.
14. Can, V.; Abdurrahmanoglu, S.; Okay, O. *Polymer* 2007, 48, 5016.
15. Gundogan, N.; Melekaslan, D.; Okay, O. *Macromolecules* 2002, 35, 5616.
16. Sayil, C.; Okay, O. *Polymer* 2001, 42, 7639.
17. Flory, P. J. *Principles of Polymer Chemistry*; Cornell University Press: Ithaca, NY, 1953.
18. Treloar, L. R. G. *The Physics of Rubber Elasticity*; University Press: Oxford, 1975.
19. Gundogan, N.; Okay, O.; Oppermann, W. *Macromol Chem Phys* 2004, 205, 814.
20. Kizilay, M. Y.; Okay, O. *Macromolecules* 2003, 36, 6856.
21. Aubry, T.; Bossard, F.; Moan, M. *Langmuir* 2002, 18, 155.
22. Argillier, J.-F.; Audibert, A.; Lecourtier, J.; Moan, M.; Rousseau, L. *Colloids Surf A* 1996, 113, 247.
23. Durmaz, S.; Okay, O. *Polymer* 2000, 41, 3693.
24. Mark, J. E.; Erman, B. *Rubberlike Elasticity. A Molecular Primer*; Cambridge University Press: Cambridge, 2007.
25. Okay, O.; Durmaz, S. *Polymer* 2002, 43, 1215.
26. Hirokawa, T.; Tanaka, T. *J Chem Phys* 1984, 81, 6379.
27. Nicolai, T.; Cocard, S. *Eur Phys J* 2001, E5, 221.
28. Nicolai, T.; Cocard, S. *J Colloid Interface Sci* 2001, 244, 51.
29. Baghdadi, H. A.; Sardinha, H.; Bhatia, S. R. *J Polym Sci B Polym Phys* 2005, 43, 233.
30. Zebrowski, J.; Prasad, V.; Zhang, W.; Walker, L. M.; Weitz, D. A. *Colloids Surf A* 2003, 213, 189.
31. Pozzo, D. C.; Walker, L. M. *Colloids Surf A* 2004, 240, 187.